Proc. Natl. Acad. Sci. USA
Vol. 94, pp. 9637–9642, September 1997
Biophysics

The 2.0-Å resolution crystal structure of a trimeric antibody fragment with noncognate V_H–V_L domain pairs shows a rearrangement of V_H CDR3

XUE Y. PEI*, PHILIPP HOLLIGER*, ALEXEY G. MURZIN*, AND ROGER L. WILLIAMS*†‡

*Centre for Protein Engineering and †Laboratory of Molecular Biology, Medical Research Council Centre, Hills Road, Cambridge CB2 2QH, United Kingdom

Communicated by Max F. Perutz, Medical Research Council, Cambridge, United Kingdom, June 20, 1997 (received for review April 2, 1997)

ABSTRACT **The 2.0-Å resolution x-ray crystal structure of a novel trimeric antibody fragment, a "triabody," has been determined. The trimer is made up of polypeptides constructed in a manner identical to that previously described for some "diabodies": a V_L domain directly fused to the C terminus of a V_H domain—i.e., without any linker sequence. The trimer has three Fv heads with the polypeptides arranged in a cyclic, head-to-tail fashion. For the particular structure reported here, the polypeptide was constructed with a V_H domain from one antibody fused to the V_L domain from an unrelated antibody giving rise to "combinatorial" Fvs upon formation of the trimer. The structure shows that the exchange of the V_L domain from antibody B1-8, a V_λ domain, with the V_L domain from antibody NQ11, a V_κ domain, leads to a dramatic conformational change in the V_H CDR3 loop of antibody B1-8. The magnitude of this change is similar to the largest of the conformational changes observed in antibody fragments in response to antigen binding. Combinatorial pairing of V_H and V_L domains constitutes a major component of antibody diversity. Conformationally flexible antigen-binding sites capable of adapting to the specific CDR3 loop context created upon V_H–V_L pairing may be employed by the immune system to maximize the structural diversity of the immune response.**

The antigen-binding site in antibodies is formed by the hypervariable loop regions (complementarity-determining regions, CDRs) of V_H and V_L domain pairs to yield a continuous surface mounted on a rigid scaffold provided by the framework regions of these domains. The ultimate diversity of antigen binding is determined by the structural diversity of this surface. From extensive analysis of structures of antibody fragments, it is clear that there is only a small set of "canonical" main-chain loop conformations for five of the six CDRs (1, 2). However, CDR3 of the V_H domain, located at the center of the antigen-binding site, has defied attempts at classification due to its large variability in length and sequence, resulting from the junctional diversity generated in somatic V_H gene assembly. Furthermore, a range of conformational changes in antigen-binding sites can occur upon antigen binding (3–8). These changes range from minor side-chain adjustments to major rearrangements in the main-chain loop conformations of V_H CDR3, as well as to changes in the relative orientation of the V_H and V_L domains (3). Furthermore, the biphasic kinetics of some antibodies in response to antigen binding suggest that there is conformational heterogeneity even prior to antigen binding (9, 10).

A fundamental component of antibody diversity arises from random V_H–V_L pairings. "Promiscuous" V_H–V_L pairings have also been observed in phage-displayed antibody libraries and have been exploited for affinity maturation *in vitro* (11) or "humanizing" antibodies (12, 13). It has been anticipated that novel V_H–V_L pairings could influence the conformations of the CDR loops (14). We have determined the structure of an Fv consisting of a V_H domain from one antibody paired with a V_L domain from an unrelated antibody. This structure shows a large rearrangement of the antigen-binding region of the V_H domain and reinforces that the expressed structural diversity is not simply related to the product of the sequence diversity of the V_H and V_L domains considered independently.

An unrelated but important objective of our work was to show that single chain Fv fragments with very short linkers between the V_H and V_L domains (zero residues in this instance) can form stable trimers. Previously, we described the structure of a dimeric antibody construct known as a "diabody" (15). In such a construct V_H and V_L domains are fused to each other with a linker sequence too short to permit intramolecular pairing of the domains, forcing formation of dimers. In several diabody preparations, we have noticed higher-order oligomers. For the B1-8/NQ11 construct in which the V_H domain of B1-8 is directly fused to the N terminus of the V_L domain of NQ11, the preparation consisted predominantly of oligomers with a gel-filtration estimated size consistent with a trimer. We report here the structure of a trimeric antibody fragment.

MATERIALS AND METHODS

Vector Construction. An antibody fragment was constructed so that the V_H domain of antibody B1-8 was directly fused to the V_L domain of antibody NQ11 as illustrated in Fig. 1. Because the V_H and V_L domains are directly fused to each other, it is not sterically possible for the V_H and V_L domains in a single polypeptide to pair with each other. Consequently, the polypeptides form oligomers in which the V_H–V_L pairing is achieved intermolecularly (16–19). This type of multivalent antibody fragment has been referred to as a diabody (15, 17), although dimeric, trimeric, and higher-order multimers can be isolated (16–19).

Expression and Purification of Antibody Fragments. The multivalent antibody fragment B1-8/NQ11 was expressed in *Escherichia coli*. The protein was purified from culture supernatant using three chromatagraphic steps: Ni^{2+}-NTA agarose (Qiagen, Chatsworth, CA) affinity purification, gel filtration with a HiLoad 16/60 Superdex 75 column (Pharmacia) equilibrated with 20 mM Tris·HCl (pH 8.0), 0.1 M NaCl, and finally a salt gradient on a MonoQ HR 5/5 column equilibrated in 20 mM Tris·HCl (pH 8.0). Gel filtration analysis indicated that

The publication costs of this article were defrayed in part by page charge payment. This article must therefore be hereby marked "*advertisement*" in accordance with 18 U.S.C. §1734 solely to indicate this fact.

Abbreviation: CDR, complementarity-determining region.

Data deposition: The atomic coordinates and structure factors have been deposited in the Protein Data Bank, Biology Department, Brookhaven National Laboratory, Upton, NY 11973 (reference 1nqb).

‡To whom reprint requests should be addressed. e-mail: rlw@mrc-lmb.cam.ac.uk.

a.

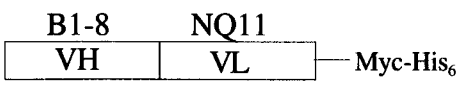

b.

VH domain (B1-8)

```
1       10          20          30          40          50 52a      59      65  69          79
1       10          20          30          40          50  53      60      66  70          80
                                    CDR1                        CDR2
QVQLQQSGAE LVKPGASVKL SCKASGYTFT SYWMHWVKQR PGRGLEWIGR IDPNSGGTKY NEKFKSKATL TVDKPSSTAY
                                       H1    *   *     ** *       H2

 82abc  86          95   100abc103          113
        90          99           110         120
                    CDR3
MQLSSLTSED SAVYYCARYD YYGSSYFDYW GQGTTVTVSS
             *   *  H3 ***** *  *
```

VL domain

```
        1       10          20        27abc def     34          44          54          64
                10          20                      39          49          59          69
                                        CDR1                                CDR2
NQ11,κ DIELTQTPLS LPVSLGDQAS ISCRSSQSIV HS-NGNTYLE WYLQKPGQSP KLLIYKVSNR FSGVPDRFSG
                                        L1                              L2

        1         9         20        27abc 29      34          44          54          64
                  9         19          29 31       36          46          56          66
B1-8,λ QAVVTQE-SA LTTSPGETVT LTCRSSTGAV TT---SNYAN WVQEKPDHLF TGLIGGTNNR APGVPARFSG
                                                  * *  * *   ***  *  **  * **

                  74          84          94          104  108
                  79          89          99          109  113
                                        CDR3                        Myc tag     His tag
NQ11,κ SGSGTDFTLK ISRVEAEDLG VYYCFQGSHV PYTFGGGTKL EIKR AAAEQKLISEEDLNGAAHHHHHH
                                          L3

                  74          84          94          104
                  76          86          96          106  110
B1-8,λ SLIGDKAALT ITGAQTEDEA IYFCALWYSN HWVFGGGTKL TVLE
                                    *       * ** *
```

FIG. 1. (*a*) A schematic of the B1-8/NQ11 construct. The polypeptide chain of the homotrimer is composed of an N-terminal V_H domain from antibody B1-8 (37) fused directly to a C-terminal V_L domain (κ-type) from antibody NQ11 with a *myc* tag and a $(His)_6$ tag at the C terminus. (*b*) The sequence of the triabody B1-8/NQ11. The CDRs are indicated by bars above the sequence. The hypervariable loops as defined by Chotia and Lesk (1) are indicated by bars below the sequence. The sequence of the cognate V_L domain (λ-type) from B1-8 is indicated below the sequence of the V_L domain from NQ11. The sequential sequence numbering used throughout the text and in the Protein Data Bank entry is on the line closest to the sequence. The numbering of Kabat *et al.* (38) is shown as the uppermost line of each sequence. The residues that are involved in V_H–V_L interface contacts (closer than 4.0 Å) are shown in bold for B1-8/NQ11 and by asterisks below the sequence for B1-8.

dimers, trimers, and higher-order oligomers are present. The trimeric fraction was pooled and applied to the MonoQ. The protein was concentrated to 18.7 mg/ml and stored at 4°C. Our purification protocol and structure determination focused on a trimeric or "triabody" species.

Crystallization. Initial small crystals appeared at 4°C in 30% 2-propanol, 0.1 M Na cacodylate (pH 6.5), and 0.2 M Na citrate. Subsequently, pre-equilibrated drops were micro-seeded. A typical crystal had dimensions of 0.2 mm × 0.2 mm × 0.1 mm. The crystals have R3 symmetry with unit cell dimensions $a = 136.32$ Å, $c = 74.8$ Å. The Matthews coefficient (V_M) of the crystals is 2.4 Å^3/Da.

X-Ray Diffraction Data Collection. Data from a single crystal were collected at the Daresbury Synchrotron Station 9.6 at a wavelength of 0.882 Å with a MAR-Research (Hamburg, Germany) 300-mm image plate. Data were collected to a resolution of 1.9 Å. The crystal for data collection was flash frozen in a nitrogen cold stream at 95 K. The freezing solution was the same solution as used for growing the triabody crystals with the addition of 20% (wt/vol) 2-methyl-2,4-pentanediol. Diffraction data were processed and refined with the program MOSFLM (20). Data sorting, scaling and merging were done with the CCP4 package (21). There were a total of 95,579 observations of 33,839 unique reflections giving an average redundancy of 2.8. Data were 96.6% complete to 1.9 Å. The overall R_{sym} was 0.053 based on intensities with an R_{sym} of 0.174 for the data from 2.0 Å to 2.05 Å.

Initial Phase Determination. Initial phases were obtained by molecular replacement method using the program AMORE

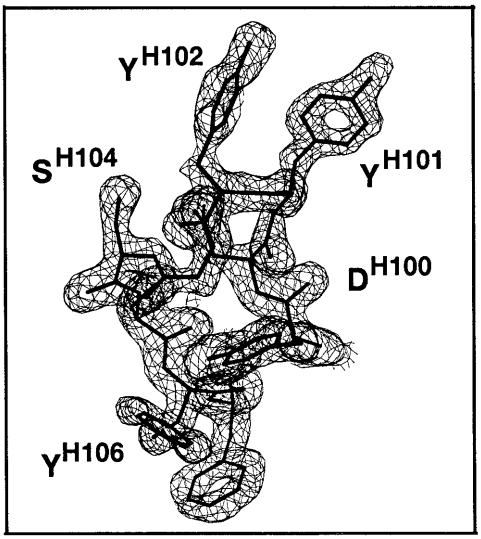

FIG. 2. A simulated annealing OMIT difference electron density map contoured at 3σ for V_H CDR3 of the B1-8/NQ11 triabody [drawn with BOBSCRIPT (R. Esnouf, personal communication), a modified version of MOLSCRIPT (39)].

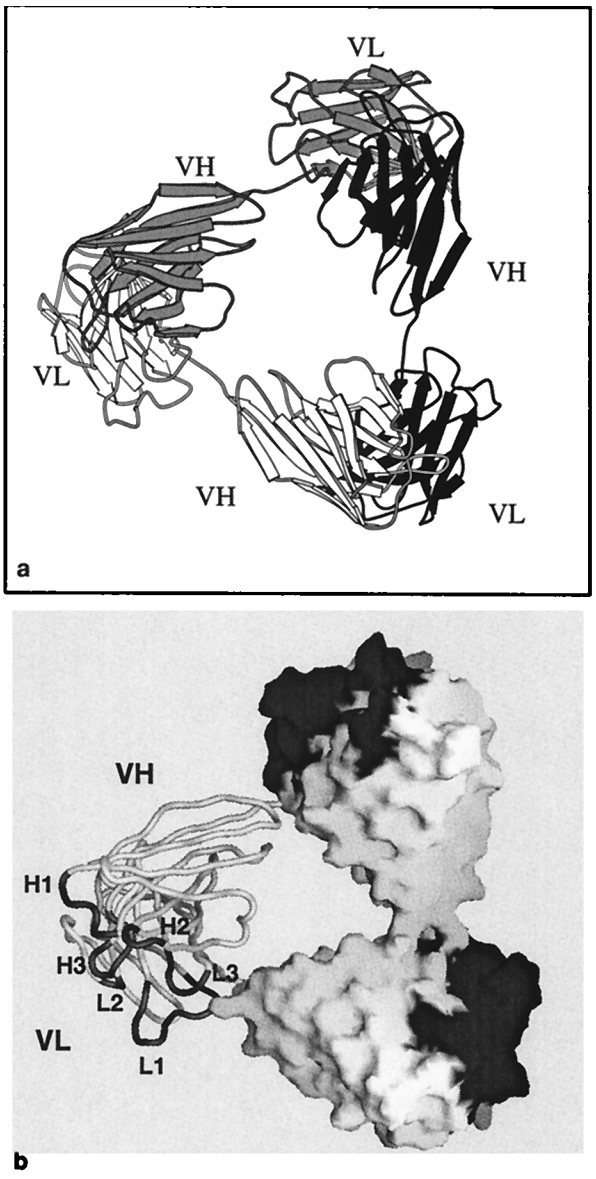

FIG. 3. The overall structure of the triabody. (*a*) Three polypeptides in one triabody are related to each other by crystallographic symmetry and are rendered in different shades of gray. The triabody has three Fv heads, each consisting of a V_H domain from one polypeptide paired with the V_L domain from a neighboring polypeptide. (*b*) A view of a triabody with the molecular surface superimposed on two of the Fv heads in the triabody and the third Fv head shown in worm representation. The CDRs of each Fv head are shaded dark gray.

(22). An initial rotation function was calculated using search models derived from a library of 37 Fv structures. The 10 highest rotation function solutions for each Fv were used for translation function searches. Monoclonal antibody fragment JE142 (Protein Data Bank entry 1jel) yielded the highest correlation coefficient (21.9%) and lowest *R* factor (51.8%) and was used for the next step of the analysis. This initial rotation/translation solution was refined as a rigid-body and was subsequently fixed for a second round of the translation function searches to locate a second molecule. In the second round of the translation function searches, all of the 37 Fv structures were again used. The second round of translation function searches yielded a correlation coefficient of 29.1% and an *R* factor of 49.8%. Again, JE142 was the Fv that gave the strongest signal. The two molecules in the asymmetric unit were refined as four rigid-bodies (two V_H and two V_L domains). This yielded a correlation coefficient of 61.3% and *R* factor of 36.5%.

Structure Refinement. The structure was refined using data to 2.0-Å resolution. Unrestrained refinement was carried out with the program ARP (23) to generate an electron density map that was used for initial model building. An initial model was built using the program O (24). Noncrystallographic symmetry restrained positional and temperature factor refinement were carried out with the program X-PLOR. A few cycles of X-PLOR (25) least-squares refinement (using all data not flagged as "free" from 6.0 Å to 2.0 Å resolution, 31,030 reflections) alternated with model rebuilding into difference electron density maps produced as a result of unrestrained ARP refinement, yielded an *R* factor of 0.235 and a free *R* factor of 0.262 (using 5% of the data, 1,649 reflections). After switching off the NCS restraints, the *R* factor was 0.187 with a free *R* factor of 0.230. Simulated annealing with X-PLOR did not improve the free *R* factor. For one molecule in the asymmetric unit, residues 101–108 of the V_H domain are well defined (Fig. 2). For the other molecule in the asymmetric unit, this region is disordered. The *myc* and $(His)_6$ tags at the C terminus of the polypeptide are not visible for either of the molecules in the asymmetric unit. The junction between the N-terminal V_H and C-terminal V_L domains is well ordered and clearly discernible for both molecules in the asymmetric unit. The electron density is disordered for the main-chain in region Pro^{H41} to Arg^{H43} of both polypeptides in the asymmetric unit. The model has good stereochemistry as evaluated by PROCHECK (26). Root-mean squared deviations from ideal geometry are 0.008 Å, 1.41°, and 26.9° for bond lengths, bond angles, and dihedral angles, respectively.

RESULTS AND DISCUSSION

The Structure of a Trimeric, Combinatorial Antibody Fragment. The overall fold of the antibody fragment is of a type that has been referred to as a domain-swapped trimer (27). The trimer has three Fv heads with the polypeptides in the trimer arranged in a cyclic head-to-tail fashion. The V_H domain of each polypeptide pairs with the V_L domain of a neighboring polypeptide in the trimer giving rise to three antigen-binding sites (Fig. 3). Monomers of single chain Fvs with short linker sequences between the V_H and V_L domains are not functional and constitute little if any of the material expressed. However,

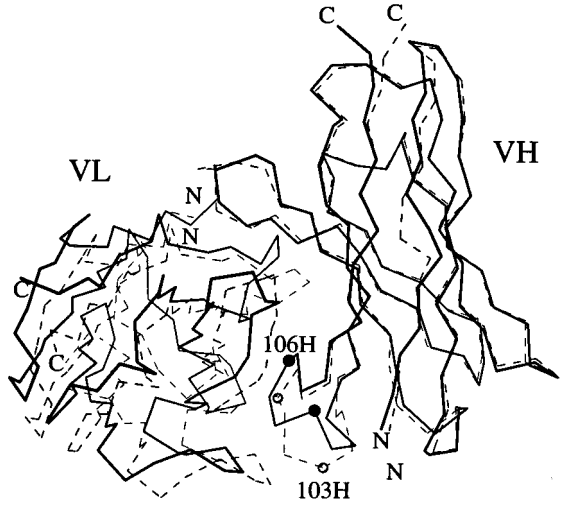

FIG. 4. A comparison of the V_L–V_H orientations of the B1-8 (dashed lines) and B1-8/NQ11 (solid lines) Fvs. The C^α values of the B1-8 V_H framework were superimposed on the B1-8/NQ11 V_H framework. The C^α positions of residues Gly^{H103} and Tyr^{H106} are indicated by spheres (white for B1-8 and black for B1-8/NQ11).

the structure of NQ11/B1-8 and the structure of a diabody reported previously (15) show that this type of antibody fragment readily forms domain-swapped dimers and trimers.

The present structure may be used as a blueprint for the design and construction of trivalent or even trispecific antibody fragments. Triabodies could bind three different or identical epitopes on the same molecule leading to higher specificities and higher functional affinities. Furthermore, by cross-linking three different types of antigens trispecific triabodies might, in principle, be useful immunotherapeutic agents by retargeting resting cytotoxic lymphocytes in a manner that has been demonstrated for other trispecific antibody fragments (28, 29). However, because of random pairing in a triabody system expressing three different polypeptides, only a small fraction of correctly paired, trispecific triabodies would be produced. The fraction of trispecific triabody might be improved by engineering specificity into the V_H–V_L domain interface as has been described for diabodies (30).

The polypeptide forming the trimer used in this study has a Vκ domain from the NQ11 anti-hapten phOx (2-phenyl-5-oxazolone) antibody fused to the V_H domain from an unrelated antibody, a B1-8 anti-hapten NIP (4-hydroxy-5-iodo-3-nitrophenyl acetyl) antibody. Although the "combinatorial" Fvs in the triabody we have crystallized are not capable of binding either of the haptens for which the parental antibodies were specific, they have allowed us to examine the influence of the V_L domain on the conformations of the CDRs of the V_H domain.

The Effect of Exchanging One V_L Domain for Another on the V_H Conformation. The structure of Fv B1-8 fragment had been solved previously both in the presence and absence of antigen (T. Simon and K. Henrick, personal communication). The structure of a very closely related NIP-binding Fab, N1G9, which differs by only one conservative replacement in the V_H domain (V116L), has also been determined both in the presence and absence of antigen (31) (Protein Data Bank entries 1 ngp and 1 ngq) and these four structures are nearly identical to each other. We have compared the structure of the B1-8 V_H domain paired to the B1-8 V_λ chain with the structure of it paired to the V_κ domain from NQ11. Inspection of the combinatorial B1-8/NQ11 Fv structure shows that substitution of one V_L domain for another had little influence on the conformations of the first two hypervariable loops of the V_H domain but had a profound influence on V_H CDR3 with deviations of 0.17 Å, 0.15 Å, and 1.8 Å for H1, H2, and H3, respectively.

The triabody context *per se* in which the combinatorial Fvs were expressed does not appear to have an influence on the conformation of the CDRs. As was observed for a diabody (15), both the V_H and V_L domains in each Fv head have a conformation similar to those of other antibody fragments having the same canonical classes of hypervariable regions. The main-chain rms deviation between the V_H domains of the triabody B1-8/NQ11 and the Fv B1-8 is only 0.44 Å. The profound difference in the conformation of CDR3 is largely due to conformational changes in the triabody caused by differences in V_H–V_L packing arising as a consequence of exchanging one V_L domain for another unrelated one.

Disposition of the V_H Domain Relative to the V_L Domain. Associated with the exchange of one V_L domain for another unrelated one is a pronounced change in the relative orientation of the V_H and V_L domains. The relative shift of the V_L domain in B1-8/NQ11 in comparison with Fv B1-8 is a 9.1° rotation around an axis perpendicular to the V_H–V_L interface and 2.4-Å translation (Fig. 4). The change in orientation that we have observed upon exchanging one V_L domain for an unrelated one is similar to the largest of the antigen induced interdomain movements that have been reported: 16° for the HIV-1 neutralizing Fab 50.1 and 7.5° for the anti-DNA Fab BV04 (32).

The residues involved in the V_H–V_L interface are quite common in comparison with other antibodies (Table 1). Among these interface residues are most of the residues of the V_H CDR3 loop. The extent of the V_H–V_L interface is similar to the interface found in Fv B1-8 and fairly large (1,720 $Å^2$) relative to other antibodies (solvent accessible surface area buried in the interface calculated using a 1.4-Å probe and the default atomic radii of the program GRASP). Most of the V_H–V_L interactions in B1-8 involve residues in L3 and H3 (31). The residues of the V_H domain that are involved in the interface of B1-8/NQ11 are generally the same residues involved in the B1-8 interface (Fig. 1). Those that differ between B1-8/NQ11 and B1-8 are residues packing against CDR3 of the V_L domain. These differences in packing are not surprising. All of the mouse V_λ domains whose structures have been determined, including B1-8, have similar L3 conformations, and these differ from canonical "type-1" L3 conformation found in V_κs such as that of B1-8/NQ11 (1).

Rearrangement of the V_H CDR3 Loop. The V_H CDR3 loop, residues 99^H–109^H, of the triabody has its tip twisted with respect to its conformation in Fv B1-8 (Fig. 5). The twist of the loop is accomplished by a flip of the main-chain dihedral angles for residues half-way between the base and the tip, Gly^{H103}, Ser^{H104}, and Ser^{H105} [sequential triabody numbering (Fig. 1)] (Table 2). The conformational change in H3 results in main-chain deviations of up to 5.6 Å (C^α of Gly^{H103}) and a maximal side-chain deviation of 13.9 Å (OH of Tyr^{H106}). The

Table 1. Framework residues (40) found at the V_L–V_H interface (sequential B1-8/NQ11 numbering) for several antibodies whose structures have been reported

	V_L domain									V_H domain								
Antibody (PDB entry)	39	41	43	49	51	92	94	101	103	35	37	39	45	47	95	97	107	110
B1-8/NQ11 triabody	E	Y	Q	P	L	Y	F	Y	F	H	V	Q	L	W	Y	A	F	W
B1-8	N	V	E	F	G	F	A	W	F	H	V	Q	L	W	Y	A	F	W
JE142 (1jel)	E	Y	Q	P	L	Y	F	Y	F	H	V	Q	L	W	Y	A	F	W
ANO2 (1baf)	Y	Y	Q	P	L	Y	Q	I	F	N	I	Q	L	W	Y	T	F	W
HIL (8fab)	Y	Y	Q	P	M	Y	Q	S	F	H	V	Q	L	W	Y	A	F	W
A/CYC1 (likf)	N	Y	Q	V	L	F	Q	P	F	Y	V	Q	L	W	Y	T	F	W
D1.3 (1vfa)	A	Y	Q	P	L	Y	Q	R	F	N	V	Q	L	W	Y	A	L	W
MCPC603 (1mcp)	A	Y	Q	P	L	Y	Q	L	F	E	V	Q	L	W	Y	A	F	W
NEW (7fab)	K	Y	Q	P	L	Y	Q	R	F	T	V	Q	L	W	Y	A	I	W
4-4-20 (4fab)	R	Y	Q	P	V	F	S	W	F	N	V	Q	L	W	Y	T	M	W
C3 (1fpt)	H	Y	Q	P	L	F	S	Y	F	Q	I	Q	L	W	F	A	F	W
NC6.8 (1cgs)	H	Y	Q	P	L	F	S	Y	F	E	V	E	L	W	Y	T	M	W
L5MK16 diabody (11mk)	H	Y	K	P	L	F	S	F	F	E	V	Q	L	W	Y	A	L	W

PBD, Protein Data Bank.

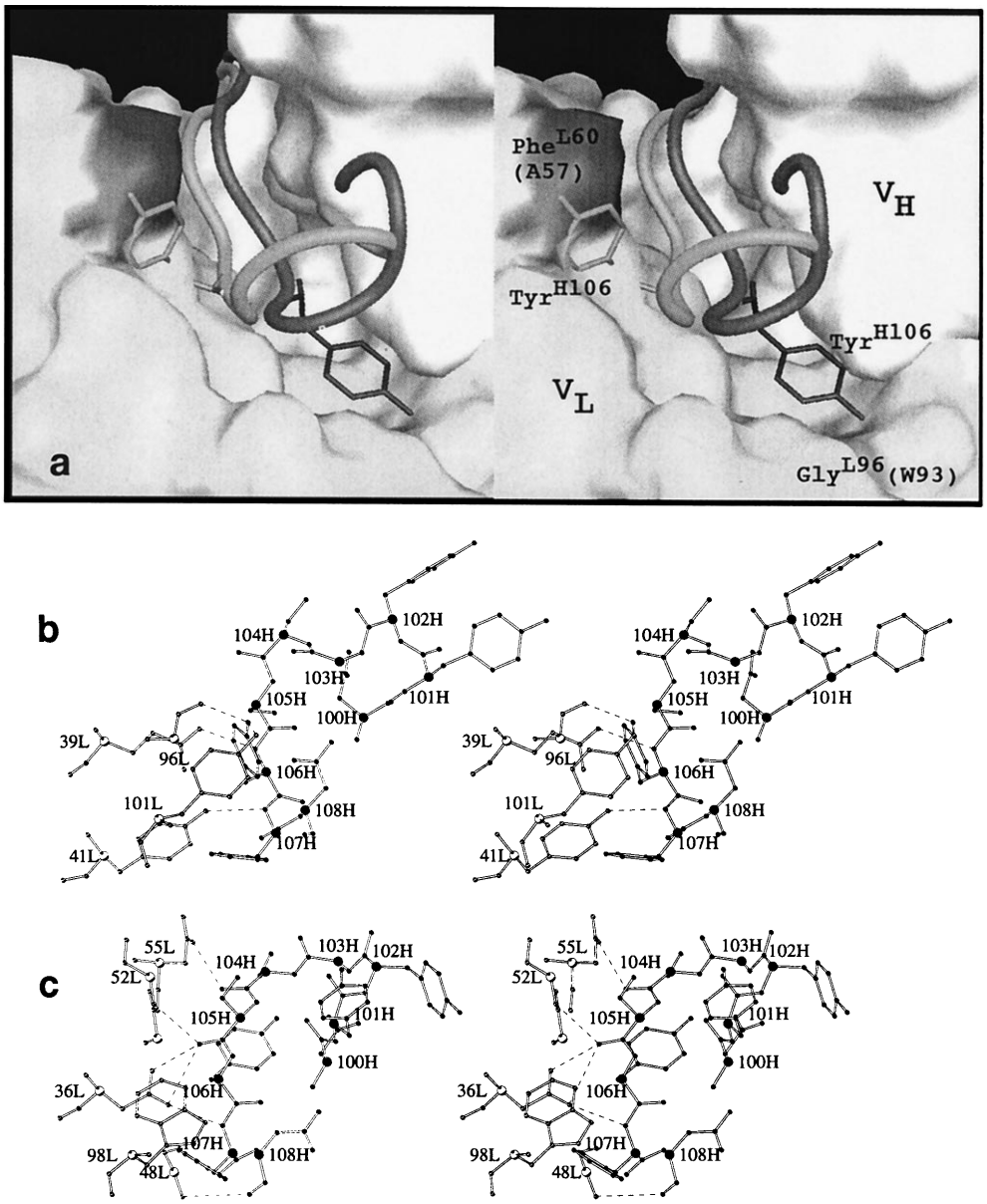

FIG. 5. Stereoview comparisons of the H3 loops in B1-8 and B1-8/NQ11. (*a*) A worm representation of the H3 loop in B1-8 (shaded lighter) superimposed on the H3 loop of B1-8/NQ11 (shaded darker). The molecular surface shown is that of the B1-8/NQ11 model with the H3 loop omitted. The surface of the V_H domain is white and the general surface of the V_L domain is light gray. The surface of Phe^{L60} is shaded dark. The analogous residue in B1-8 is Ala^{L57} that leaves space to accommodate the side chain of Tyr^{H106} (shown in stick representation) in the B1-8 Fv. The presence of Gly^{L96} (shaded) leaves space to accommodate the side chain of Tyr^{H106} in B1-8/NQ11. The analogous volume in B1-8 is occupied by Trp^{L93}. (*b*) The H3 loop of B1-8/NQ11 and its interaction with V_κ residues. The C^α positions are indicated with larger spheres. V_L atoms are shown as white spheres and V_H atoms as black spheres. (*c*) The B1-8 H3 loop and its interactions with the V_λ domain.

magnitude of this rearrangement is similar to the largest of the conformational changes induced by antigen binding (33).

Table 2. A comparison of the main-chain torsion angles for the H3 loop of B1-8/NQ11 and B1-8 antibodies

	B1-8/NQ11		B1-8		Difference	
Residue	ϕ	ψ	ϕ	ψ	$\Delta\phi$	$\Delta\psi$
Tyr-101	−55	−35	−65	−46.8	10	12
Tyr-102	−110	11	−85	−7.1	−24	18
Gly-103	68	23	−111	−108.7	179	132
Ser-104	23	−31	−102	12.0	125	−43
Ser-105	−138	160	57	44.2	165	116
Tyr-106	−88	−59	−122	158.7	34	143
Phe-107	−116	83	−91	76.3	−25	7
Asp-108	−75	−37	−70	−55.0	−5	18

A notable consequence of the conformational change of H3 is that the side chain of Tyr^{H106} is in a radically different position than in B1-8. The change in the position of Tyr^{H106} appears to be dictated by the space available for it against the surface of the V_L domain (Fig. 5*a*). In the B1-8 structure, both in the presence and absence of antigen, Tyr^{H106} is packed against the V_L domain filling the space adjacent to Ala^{L57} [B1-8 numbering (Fig. 1)]. In the B1-8/NQ11 structure, the analogous space is occupied by Phe^{L60} and by the side chain of Tyr^{L101} from the C terminus of L3 thereby occluding Tyr^{H106} from this site. Conversely, the cavity adjacent to Gly^{L96} is filled by the side chain of Tyr^{H106} in B1-8/NQ11 whereas in B1-8, the analogous volume is occupied by the side chain of Trp^{L93}. The structures suggest that the H3 loop is able to take on very different conformations in response to the surface provided by the V_L domain and that the interactions of Tyr^{H106} may be of

central importance in determining which conformation the loop adopts. The importance of this residue in determining the conformation of the H3 loop was proposed from an analysis of the H3 loop conformations observed in known antibody structures (1). The change in conformation that we observe in exchanging a V_κ for a V_λ domain is likely the consequence of general features of the κ and λ light chains. A tryptophane residue analogous to Trp^{L93} is a feature of all of the mouse V_λ germ-line sequences. It is fairly common for V_κ sequences to have a small residue at the analogous position, and it is a pocket formed by a glycine at this position in the NQ11 V_κ domain that has allowed the side chain of Tyr^{H106} to change its position so dramatically.

The conformation of the V_H CDR3 in B1–8/NQ11 is stabilized by hydrogen bonds with residues in the framework and L3 of the V_L domain: the OH of Tyr^{H106} interacts with the side chain of Tyr^{L101} and the carbonyl oxygen of Gly^{L96}, and the amide N of Phe^{H107} interacts with the OH of Tyr^{L41}. These interactions are not present in B1-8. Instead, in the B1-8 structure, V_H CDR3 is stabilized by hydrogen bonds with the framework and hypervariable loops L1 and L2 (Fig. 5). The canonical conformation of L1 unique to mouse V_λ domains (34) makes it likely that H3–L1 interactions will be altered upon replacing a V_κ domain with a V_λ domain.

Combinatorial V_H–V_L pairing constitutes a fundamental source of antibody diversity in the immune response. However, the B1-8/NQ11 structure provides evidence that the expressed diversity is not simply related to the genetic diversity. The exchange of one variable domain for another through the process known as "receptor editing" may be an important feature of development of the Ig repertoire (35, 36). Thus a novel V_H–V_L pairing may "remodel" the binding site through conformational changes of V_H CDR3. This may abolish antigen binding, but it may also allow the immune response to escape from a dead-end antigen-binding site that cannot be improved beyond a certain limit by somatic mutation, providing a fresh start with an entirely reshaped antigen-binding site. Plasticity of the H3 loop may be an important source of diversity of antigen-binding sites and may be an important consideration for antibody design and structure prediction.

We thank O. Perisic for help with experiments and for comments on the manuscript; T. Simon and K. Henrick for providing the coordinates of B1-8; C. Chothia, A. Lesk, and G. Winter for helpful discussions; and I. Fearnley for mass spectroscopy. Daresbury synchrotron radiation source and the staff of Station 9.6 are gratefully acknowledged for their assistance. The work was supported by the MRC/DTI/ZENECA/LINK program.

1. Chothia, C. & Lesk, A. M. (1987) *J. Mol. Biol.* **196,** 901–917.
2. Chothia, C., Lesk, A. M., Tramontano, A., Levitt, M., Smith-Gill, S. J., Air, G., Sheriff, S., Padlan, E. A., Davies, D., Tulip, W. R., Colman, P. M., Spinelli, S., Alzari, P. M. & Poljak, R. J. (1989) *Nature (London)* **342,** 877–883.
3. Wilson, I. A. & Stanfield, R. L. (1993) *Curr. Opin. Struct. Biol.* **3,** 113–118.
4. Wilson, I. A. & Stanfield, R. L. (1994) *Curr. Opin. Struct. Biol.* **4,** 857–867.
5. Sheriff, S., Chang, C. Y., Jeffrey, P. D. & Bajorath, J. (1996) *J. Mol. Biol.* **259,** 938–946.
6. Rini, J. M., Schulze-Gahmen, U. & Wilson, I. A. (1992) *Science* **255,** 959–965.
7. Braden, B. C. & Poljak, R. J. (1995) *FASEB J.* **9,** 9–16.
8. Braden, B. C., Fields, B. A., Ysern, X., Goldbaum, F. A., Dall'Acqua, W., Schwarz, F. P., Poljak, R. J. & Mariuzza, R. A. (1996) *J. Mol. Biol.* **257,** 889–894.
9. Foote, J. & Milstein, C. (1991) *Nature (London)* **352,** 530–532.
10. Foote, J. & Milstein, C. (1994) *Proc. Natl. Acad. Sci. USA* **91,** 10370–10374.
11. Clackson, T., Hoogenboom, H. R., Griffiths, A. D. & Winter, G. (1991) *Nature (London)* **352,** 624–628.
12. Figini, M., Marks, J. D., Winter, G. & Griffiths, A. D. (1994) *J. Mol. Biol.* **239,** 68–78.
13. Jespers, L. S., Roberts, A., Mahler, S. M., Winter, G. & Hoogenboom, H. R. (1994) *Bio/Technology* **12,** 899–903.
14. Steipe, B., Plückthun, A. & Huber, R. (1992) *J. Mol. Biol.* **225,** 739–753.
15. Perisic, O., Webb, P. A., Holliger, P., Winter, G. & Williams, R. L. (1994) *Structure* **2,** 1217–1226.
16. Griffiths, A. D., Malmqvist, M., Marks, J. D., Bye, J. M., Embleton, M. J., McCafferty, J., Baier, M., Holliger, K. P., Gorick, B. D., Hughes-Jones, N. C., Hoogenboom, H. R. & Winter, G. (1993) *EMBO J.* **12,** 725–734.
17. Holliger, P., Prospero, T. & Winter, G. (1993) *Proc. Natl. Acad. Sci. USA* **90,** 6444–6448.
18. Nissim, A., Hoogenboom, H. R., Tomlinson, I. M., Flynn, G., Midgley, C., Lane, D. & Winter, G. (1994) *EMBO J.* **13,** 692–698.
19. Whitlow, M., Filpula, D., Rollence, M. L., Feng, S.-L. & Wood, J. W. (1994) *Protein Eng.* **7,** 1017–1026.
20. Leslie, A. G. W. (1992) *Joint CCP4 and ESF-EACMB Newsletter on Protein Crystallography* (Daresbury Lab., Warrington, U.K.), Vol. 26.
21. CCP4 (1994) *Acta Crystallogr. D* **50,** 760–763.
22. Navaza, J. (1994) *Acta Crystallogr. A* **50,** 157–163.
23. Lamzin, V. S. & Wilson, K. S. (1993) *Acta Crystallogr. D* **49,** 129–147.
24. Jones, T. A., Zou, J.-Y., Cowan, S. W. & Kjeldgaard, M. (1991) *Acta Crystallogr. A* **47,** 110–119.
25. Brünger, A. (1992) X-PLOR Manual (Yale Univ., New Haven, CT).
26. Laskowski, R. A., MacArthur, M. W., Moss, D. S. & Thornton, J. M. (1993) *J. Appl. Crystallogr.* **26,** 283–291.
27. Bennett, M. J., Schlubegger, M. P. & Eisenberg, D. (1995) *Protein Sci.* **4,** 2455–2468.
28. Jung, G., Freiman, U., Marschall, Z. V., Reisfeld, R. A. & Wilmanns, W. (1991) *Eur. J. Immunol.* **21,** 2431–2435.
29. Tutt, A., Stevenson, G. T. & Glennie, M. J. (1991) *J. Immunol.* **147,** 60–69.
30. Zhu, Z., Presta, L. G., Zapata, G. & Carter, P. (1997) *Protein Sci.* **6,** 781–788.
31. Mizutani, R., Miura, K., Nakayama, T., Shimada, I., Arata, Y. & Satow, Y. (1995) *J. Mol. Biol.* **254,** 208–222.
32. Stanfield, R. L., Takimoto-Kamimura, M., Rini, J. M., Profy, A. T. & Wilson, I. A. (1993) *Structure* **1,** 83–93.
33. Stanfield, R. L. & Wilson, I. A. (1994) *Trends Biotechnol.* **12,** 275–279.
34. Wu, S. & Cygler, M. (1993) *J. Mol. Biol.* **229,** 597–601.
35. Tiegs, S. L., Russell, D. M. & Nemazee, D. (1993) *J. Exp. Med.* **177,** 1009–1020.
36. Chen, C., Nagy, Z., Prak, E. L. & Wiegert, M. (1995) *Immunity* **3,** 747–755.
37. Bothwell, A. L., Paskind, M., Reth, M., Imanishi-Kari, T., Rajewski, K. & Baltimore, D. (1981) *Cell* **24,** 625–637.
38. Kabat, E. A., Wu, T. T., Perry, H. M., Gottesman, K. S. & Foeller, C. (1991) *Sequences of Proteins of Immunological Interest* (U.S. Department of Health and Human Services, Bethesda, MD).
39. Kraulis, P. J. (1991) *J. Appl. Crystallogr.* **24,** 946–950.
40. Chothia, C., Novotny, J., Bruccoleri, R. & Karplus, M. (1985) *J. Mol. Biol.* **186,** 651–663.